Journal of Solid State Chemistry 279 (2019) 120935

Contents lists available at ScienceDirect

Journal of Solid State Chemistry

Muon-spin relaxation and AC magnetometry study of the ferrimagnet $LaSr_2Cr_2SbO_9$

E.C. Hunter [a], P.D. Battle [a,*], S.J. Blundell [b], C.V. Topping [b], F.K.K. Kirschner [b], F. Lang [b]

[a] Inorganic Chemistry Laboratory, University of Oxford, South Parks Road, Oxford, OX1 3QR, UK
[b] University of Oxford, Department of Physics, Clarendon Laboratory, Parks Road, Oxford, OX1 3PU, UK

ARTICLE INFO

Keywords:
Muon spin relaxation
AC magnetometry
Domain wall motion
Ferrimagnetic perovskite

ABSTRACT

AC susceptibility and muon spin relaxation data have been collected from a polycrystalline sample of $LaSr_2Cr_2SbO_9$, a perovskite-like compound wherein the unequal distribution of Cr^{3+} and Sb^{5+} cations over two crystallographically-distinct six-coordinate B sites results in the onset of ferrimagnetism at ~150 K. The data are used to elucidate the dynamics of the ferrimagnetic domain walls, thought to lie in Sb-rich regions, and suggest an energy barrier of ~0.13 eV to their motion. The muon data confirm that the ferrimagnetic order is a true bulk phenomenon. The behaviour of this material is briefly compared to that of Ni^{2+}- based relaxor ferromagnets.

1. Introduction

A simple cubic perovskite has the general formula ABO_3 where A is usually a relatively large divalent or trivalent cation and B is a smaller transition-metal or p-block cation. The symmetry of the structure is lowered if the BO_6 octahedra tilt, rotate or distort and it can be modified further when multiple cation species occupy the six-coordinate sites. If the different species vary significantly in size and/or charge, they will have different coordination requirements and will consequently occupy the six-coordinate sites in an ordered manner. When such two species are present in a 1:1 ratio the compound is better formulated as a double perovskite, $A_2BB'O_6$. These commonly have monoclinic or triclinic symmetry [1,2], with two crystallographically-distinct six-coordinate sites present in a 1:1 ratio within the unit cell. $La_3Ni_2SbO_9$ also adopts this structure despite the 2:1 ratio of six-coordinate cations [3], although other $A_3B_2B'O_9$ perovskites, such as $Ba_3Ta_2ZnO_9$, adopt structures wherein the two B sites are present in a 2:1 ratio [4]. The B-site cations in $La_3Ni_2SbO_9$ order such that one site is fully occupied by Ni^{2+} and the other by a random distribution of 33% Ni^{2+} and 67% Sb^{5+}. Given that Sb^{5+} is diamagnetic, the imbalance of paramagnetic Ni^{2+} across the two sites was expected to give rise to ferrimagnetic order and indeed in magnetometry studies a spontaneous magnetisation was observed below ~105 K. However, our initial neutron diffraction experiments failed to identify any magnetic Bragg scattering. When the experiments were repeated in an applied magnetic field, magnetic Bragg scattering consistent with G_z-type ferrimagnetic order was observed with the proportion of the sample undergoing ferrimagnetic order increasing as a function of applied field [5]. High-resolution transmission electron microscopy revealed variations in the Ni/Sb distribution across the crystallite and it was proposed that the Sb-rich regions act as domain walls that magnetically isolate ferrimagnetic microdomains; these microdomains only become co-aligned upon the application of an applied field. By analogy to relaxor ferroelectrics we described $La_3Ni_2SbO_9$ as a relaxor ferromagnet. We have since looked for relaxor ferromagnetic behaviour in other $A_3B_2B'O_9$ compounds, investigating nickel-containing compositions such as $La_3Ni_2B'O_9$ (B=Nb and Ta) [6] and $CaLn_2Ni_2WO_9$ (Ln = La, Pr, Nd) [7] as well as some iron- or chromium-containing analogues [8,9]. The synthesis of Cr^{3+}-containing $LaSr_2Cr_2SbO_9$ allowed us to investigate [10] the effect of changing the magnetic superexchange interactions from being σ-mediated to π-mediated. There was a high degree of cation order over the two B sites with one containing 87% Cr and the other only 46% Cr. The resulting imbalance of paramagnetic cations gave rise to a spontaneous magnetisation below ~150 K, *i.e.* this compound showed the behaviour we had expected from $La_3Ni_2SbO_9$. We found that $LaSr_2Cr_2SbO_9$, unlike $La_3Ni_2SbO_9$, exhibited clear magnetic Bragg scattering in powder neutron diffraction experiments conducted at 5 K in the absence of an applied field. This scattering could be attributed to long-range G_z-type ferrimagnetic order. However, the refined ordered Cr^{3+} moment at 5 K was low at 2.17(1) μ_B, suggesting that only 83.5(4) % of the sample was involved in the long-range magnetic order. Furthermore, DC magnetometry showed that the magnetic transition had a significant temperature width and AC susceptibility data suggested that

* Corresponding author.
E-mail address: peter.battle@chem.ox.ac.uk (P.D. Battle).

https://doi.org/10.1016/j.jssc.2019.120935
Received 30 July 2019; Received in revised form 2 September 2019; Accepted 3 September 2019
Available online 4 September 2019

the decoupled spins behaved in a spin-glass-like manner. Here we report the results of further AC magnetometry and muon spin relaxation (μSR) measurements on $LaSr_2Cr_2SbO_9$ that allow us to clarify the interpretation of the magnetic properties. The results are compared to those from related experiments conducted on analogous nickel-containing compositions.

2. Experimental

A dark-brown, polycrystalline sample of $LaSr_2Cr_2SbO_9$ was synthesised using the traditional ceramic method, as described previously [10]. The sample used for this study came from the same batch that had been characterised by powder x-ray and neutron diffraction, magnetometry and electron microscopy.

AC magnetometry data were collected using a Quantum Design SQUID magnetometer. A 37.8 mg polycrystalline sample of $Sr_2LaCr_2SbO_9$ was cooled in zero applied field to 5 K and the AC susceptibility was measured on warming the sample through the temperature range 5–130 K. A DC field of 0.3 mT and an AC field of amplitude 0.4 mT were applied on warming and data were collected at eleven different frequencies in the range 1 Hz–1 kHz.

Zero-field (ZF) μ^+SR experiments were performed on a polycrystalline sample of $LaSr_2Cr_2SbO_9$ in a Quantum Continuous Flow Cryostat on the GPS spectrometer at the Swiss Muon Source, PSI Switzerland. The sample was mounted in a silver foil packet and placed in a copper fly-past holder in order to minimise background signals due to muons stopping outside the sample. In a μ^+SR experiment an ensemble of spin-polarised muons is implanted in the target sample, where the muons typically come to rest in an interstitial position in the crystal. Once stopped, the muons Larmor precess around the local magnetic field they experience, which in turn results in a time evolution of the spin polarisation of the muon sample. The muons decay with an average life time of 2.2 μs into two neutrinos and a positron, with the positron being emitted preferentially along the instantaneous direction of the muon spin at decay. By measuring the time dependence of the positron emission directions the spin-polarisation of the muon ensemble can be determined as a function of time. This is achieved by placing detectors forward (F) and backward (B) of the initial muon polarisation direction and recording positron counts as a function of time in histograms $N_F(t)$ and $N_B(t)$. The spin-polarisation of the muon ensemble is then proportional to the decay positron asymmetry function, which is defined as $A(t) = (N_F(t) - \alpha N_B(t))/(N_F(t) + \alpha N_B(t))$ with α an experimental calibration constant. All the muon data were analysed using WiMDA [11].

3. Results

The real, χ′, and imaginary, χ′′, parts of the AC molar magnetic susceptibility of $LaSr_2Cr_2SbO_9$ for different frequencies ν are shown in Fig. 1 in SI units. In agreement with earlier measurements, both χ′ and χ′′ are frequency dependent with maxima at temperatures between 50 and 60 K for χ′ and between 60 and 80 K for χ′′. The frequency dependence is most obvious close to the temperature of the susceptibility maximum. If the observed behaviour is due to spin glass phenomena, then the temperature of the maximum of χ′ would be interpreted as a freezing temperature T_f. The Mydosh parameter [12], f, is given by $f = (\mathrm{d}\ln T_f)/(\mathrm{d}\ln\omega)$ where $\omega = 2\pi\nu$ and is found to be −0.016(1), though a similar analysis interpreting T_f as the maximum in χ′′ yields $f = 0.043(3)$. These small values are typical for spin glasses, but the negative value for the χ’ data (arising from T_f shifting to higher temperatures with decreasing ν), is highly unusual. It is more illuminating to consider the temperature dependence of the characteristic relaxation time that can be extracted from the AC data. This can be described using an Arrhenius law of the form

$$\tau = \tau_0 \exp\left(\frac{E_a}{k_B T}\right) \quad (1)$$

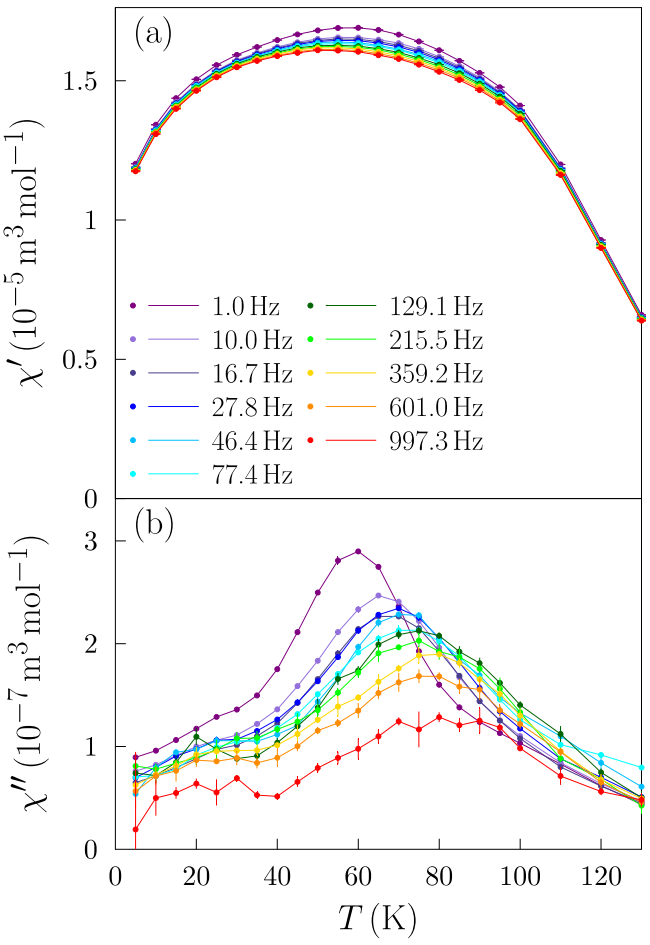

Fig. 1. – Temperature and frequency dependence of the a) real and b) imaginary parts of the molar AC susceptibility of $LaSr_2Cr_2SbO_9$ at $\mu_0 H_{d.c.} = 0.3$ mT and $\mu_0 H_{a.c.} = 0.4$ mT, collected on warming through the temperature range 5–130 K with frequencies ranging from 1 Hz to 1 kHz. Note that the AC susceptibility is reported here in SI units.

where τ_0 is the inverse attempt frequency, E_a is an energy barrier and k_B is the Boltzmann constant. Fig. 2a shows a plot of $\ln\tau$ against $1/T$, which appears to give a good fit to the Arrhenius law and yields values of

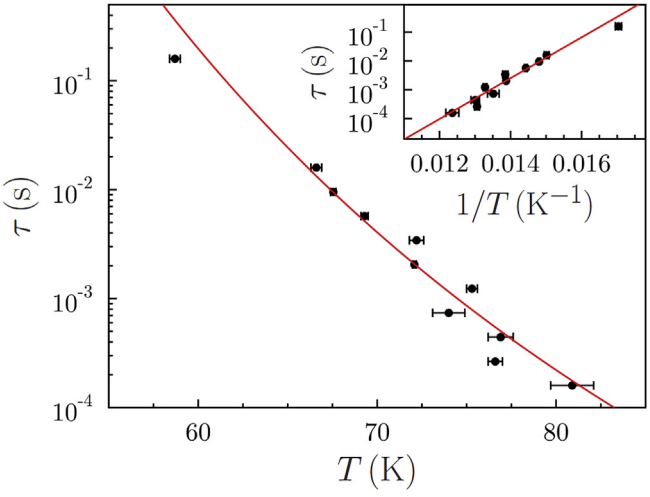

Fig. 2. – Dependence of the relaxation time, τ, of $LaSr_2Cr_2SbO_9$ on the maximum in χ′′ (T_f) at $\mu_0 H_{d.c.} = 0.3$ mT and $\mu_0 H_{a.c.} = 0.4$ mT fitted to the Arrhenius law.

$\tau_0 = 1.0(2) \times 10^{-12}$ s and $E_a/k_B = 1.5(1)\text{x}10^3$ K (corresponding to $E_a = 0.13$ eV). These values are similar to those from previous measurements on the dynamics of domain walls in ferromagnets [13] with τ_0 characteristic of thermally activated jumps, suggesting that the observed behaviour is consistent with the presence of domain walls associated with Sb-rich regions. The Arrhenius form assumes a single relaxation time and leads naturally to the Debye model [14,15]. This is likely to be an oversimplification and the next level of approximation comes from the generalised Debye model which utilises a parameter α which allows a distribution of relaxation times. In this case, the frequency-dependent susceptibility is given by

$$\chi(\omega) = \chi_S + \frac{\chi_T - \chi_S}{1 + (i\omega\tau)^{1-\alpha}} \quad (2)$$

where χ_S is adiabatic susceptibility, χ_T is the isothermal susceptibility and $0 \leq \alpha \leq 1$ [15,16]. Setting $\alpha = 0$ corresponds to no spread of relaxation times and the ideal Debye model is recovered. Fig. 3 shows the Cole-Cole (or Argand) plot of χ'' vs χ' for $LaSr_2Cr_2SbO_9$ over the temperature range 60–100 K. The data at each temperature have been fitted to the generalised Debye model using the following relation between χ'' and χ' [15,16]:

$$\chi'' = -\left(\frac{\chi_T - \chi_S}{2}\tan\frac{\pi\alpha}{2}\right) \pm \sqrt{\left(\frac{\chi_T - \chi_S}{2}\tan\frac{\pi\alpha}{2}\right)^2 + (\chi' - \chi_S)(\chi_T - \chi')} \quad (3)$$

The fits are not perfect, unsurprising as the distribution of relaxation times assumed by the generalised Debye model is unlikely to be perfectly appropriate, but the fitted values of α are consistently below 1 (with average around 0.7), demonstrating that there is some distribution of relaxation times. The picture which emerges is consistent with an ordered ground state with the AC signal arising from domain-wall motion, the distribution of timescales arising from the position-dependent constraints imposed by random variations in Sb concentration in the sample.

Further support for a magnetically ordered ground state comes from muon data. The ZF muon asymmetry function measured for $LaSr_2Cr_2SbO_9$ is shown for a series of temperatures in Fig. 4. At low temperatures a fast-decaying oscillatory signal can be observed at early times, which is indicative of long-range magnetic ordering combined with a significant relaxation of the muon spin polarisation. Below about 190 K the muon asymmetry can be fitted well in the time domain with the following function

$$A(t) = A_b + A_r(a_1 e^{-\lambda_1 t}\cos(\gamma_\mu B t + \varphi) + a_2 e^{-\lambda_2 t} + a_3), \quad (5)$$

where $\gamma_\mu = 2\pi \times 135.5$ MHz/T is the muon gyromagnetic ratio and B is the local magnetic field at the muon site. The baseline (A_b) and relaxing amplitudes (A_r) pertain to the setup of the experiment and the total number of muons stopped in the sample space and are to a good approximation constant with temperature. The remaining three terms correspond to fractions a_i of the total stopped muons experiencing different local fields. The first (a_1) term represents muons that experience a long range ordered state with additional temporal fluctuations of the magnetic field resulting in a relaxation of the spin-polarisation with rate λ_1. The second (a_2) fraction corresponds to muons that do not experience long range magnetic order but only time-varying fields which lead to a relaxation rate λ_2. The final (a_3) term allows for muons that also experience no long-range order and only very slow temporal fluctuations of their local magnetic field. Note that $a_1 + a_2 + a_3 = 1$. Above about 190 K the muon asymmetry can be well described by the function

$$A(t) = A_b + A_r(a_1 e^{-\lambda_1 t} + a_2 e^{-\lambda_2 t} + a_3), \quad (6)$$

where in comparison to equation (5) the fraction a_1 of muons now does not experience a long range ordered state, but only temporal fluctuations.

The results of fitting equations (5) and (6) to the experimental asymmetry are shown in Fig. 5. We observe that at low temperatures the majority of muons experience long-range order with local field strengths B of order 0.4 T but with a large relaxation rate λ_1. This is indicative of strong temporal variations of the long-range ordered field, which may be caused by spin fluctuations or domain boundaries moving. As the sample is warmed, the local magnetic field strength B decreases. Though the fraction a_1 of muons in magnetic regions remains roughly constant up to ~100 K, thereafter it too decreases. We can follow the magnetic signal clearly only up to 150 K, above which there is only a remnant of this which lingers, disappearing completely above about 190 K. We do not observe $B(T)$ evolving smoothly to zero, which might be evidence for a first-order transition but is more likely due to the effect of Sb-concentration variations in the sample washing out any sharp transition (and, in addition, the ordered fraction $a_1(T)$ is dropping rapidly at the same time). At higher temperature still, there is only slow spin relaxation arising from fluctuating magnetic fields at the muon site.

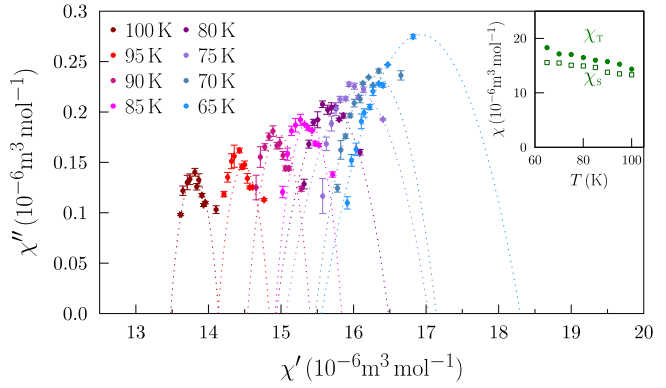

Fig. 3. – Cole-Cole plots of $LaSr_2Cr_2SbO_9$ at $\mu_0 H_{d.c.} = 0.3$ mT and $\mu_0 H_{a.c.} = 0.4$ mT at selected temperatures, fitted using the generalised Debye model. The inset shows the fitted values of χ_S (adiabatic susceptibility) and χ_T (isothermal susceptibility).

4. Discussion

The muon data provide further evidence for $LaSr_2Cr_2SbO_9$ possessing a long-range magnetically ordered ground state, which we know adopts a G_z-type ferrimagnetic structure from powder neutron diffraction measurements. However, while previously we considered the magnetic transition to occur at ~150 K, and indeed in the muSR data the magnetic signal can only be followed clearly up to 150 K, a remnant field remains up to 190 K suggesting that some Ni-rich regions of the sample begin to order at higher temperatures than initially reported. The clear oscillatory signal in the muon spin rotation data suggests that the magnetic order is a bulk phenomenon and the fraction, a_1, of muons implanted in sites that experience long-range magnetic order at 5 K is only slightly higher than the neutron diffraction derived estimate of 83.5(4) %. However, while we previously interpreted the frequency dependence of the AC susceptibility data as evidence for isolated spins decoupled from the main magnetically ordered phase, this more in-depth study shows that the low-frequency dynamics are better associated with a domain wall effect, manifesting in a temperature-dependent relaxation time corresponding to a domain-wall barrier of ~0.13 eV and a spread of relaxation times which can be attributed to small variations in Sb concentration throughout the sample. These concentration variations are also presumably responsible for the broad magnetic transition which leads to the strong temperature dependence of the ordered fraction above 100 K. The fraction of muons that only experience time varying fields, a_2, initially increases on cooling below 190 K to reach a peak at 150 K before decreasing again on cooling to 2 K. We suggest that these muons are implanted close to the domain walls, where magnetic frustration arises at the shifting boundary between ferrimagnetic domains. The number of domain walls initially increases on cooling below 190 K as lots of small ferrimagnetic domains begin to grow, precipitating from Ni-rich regions

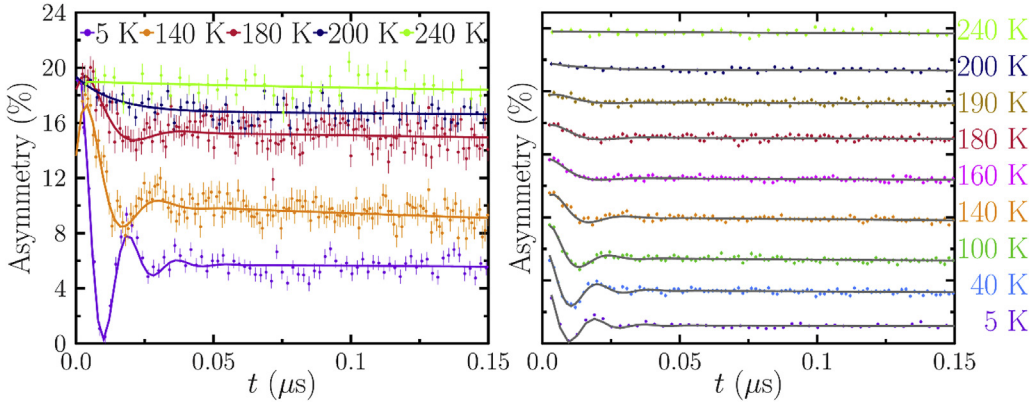

Fig. 4. – ZF muon asymmetry measured in $LaSr_2Cr_2SbO_9$ for a variety of temperatures. The solid lines represent fits according to equation (5) or (6). Note that in the right-hand panel the spectra are vertically offset from one another for readability.

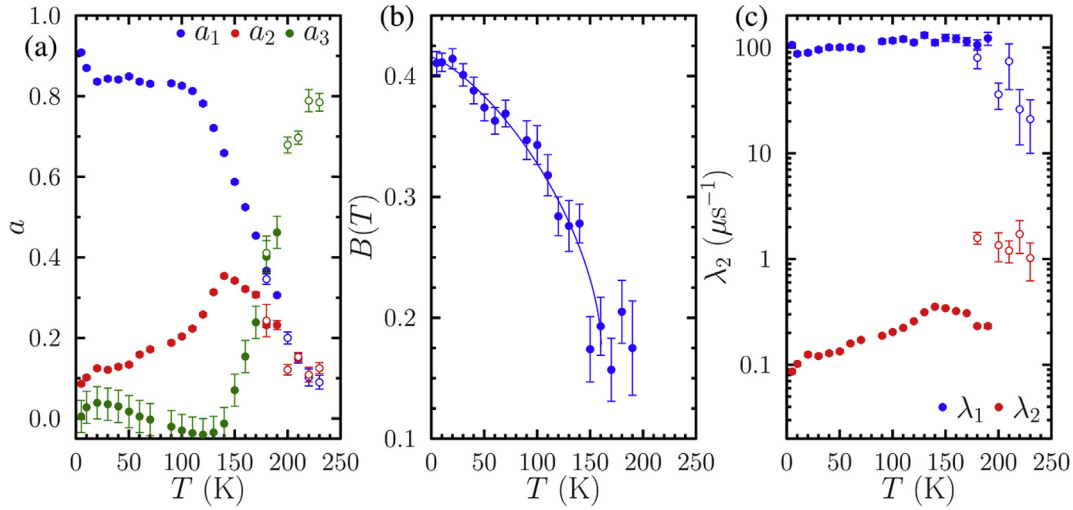

Fig. 5. – Resulting parameter values when fitting equations (5) and (6) to the measured muon asymmetry in $LaSr_2Cr_2SbO_9$. The solid blue line represents a phenomenological order parameter fit of the form $B(T) = B_0(1 - (T/T_C)^{\alpha})^{\beta}$, as a guide to the eye. (For interpretation of the references to colour in this figure legend, the reader is referred to the Web version of this article.)

of the sample. These domains increase in size and begin to merge on further cooling, increasing the proportion of magnetically ordered spins but reducing the total number of domain walls and hence the number of frustrated spins at the domain boundary. We note that there was no clear evidence for the presence of small, ordered domains above T_C in the muon data collected previously from Ni^{2+}- based relaxor compositions [6]. However, a recent neutron-scattering study [17] has elucidated the nature of the composition variations within the magnetic domains of $La_3Ni_2SbO_9$ and shown that short-range magnetic ordering does persist above the magnetic ordering temperature identified in DC magnetometry studies. The weakness of the magnetic Bragg scattering seen from that material in the absence of an applied magnetic field suggests that the domain size in $La_3Ni_2SbO_9$ is somewhat smaller than that in $LaSr_2Cr_2SbO_9$.

5. Conclusion

The experimental data reported in this paper have enabled us to interpret the magnetic properties of $LaSr_2Cr_2SbO_9$ in a consistent manner. It is clear from the muon data that the ferrimagnetic state is a bulk phenomenon, confirming the earlier observations made using magnetometry and neutron scattering.[10] The dynamics observed using AC susceptibility are most likely associated with domain walls which, on the basis of our previous work [5], we strongly suspect are associated with Sb composition variations throughout the sample. These results thus highlight the importance of cation disorder on the B site in driving the magnetic properties of double perovskites due to the interplay between structural and magnetic degrees of freedom, not only within domains but also in the domain walls.

Acknowledgments

We acknowledge financial support from the EPSRC (grant no. EP/M018954/1).

Appendix A. Supplementary data

Supplementary data to this article can be found online at https://doi.org/10.1016/j.jssc.2019.120935.

References

[1] M.T. Anderson, K.B. Greenwood, G.A. Taylor, K.R. Poeppelmeier, Prog. Solid State Chem. 22 (1993) 197–233.
[2] S. Vasala, M. Karppinen, Prog. Solid State Chem. 43 (2015) 1–36.
[3] P.D. Battle, S.I. Evers, E.C. Hunter, M. Westwood, Inorg. Chem. 52 (2013) 6648–6653.
[4] P.K. Davies, H. Wu, A.Y. Borisevich, I.E. Molodetsky, L. Farber, Annu. Rev. Mater. Res. 38 (2008) 369–401.
[5] P.D. Battle, M. Avdeev, J. Hadermann, J. Solid State Chem. 220 (2014) 163–166.

[6] C.M. Chin, P.D. Battle, S.J. Blundell, E. Hunter, F. Lang, M. Hendrickx, R.P. Sena, J. Hadermann, J. Solid State Chem. 258 (2018) 825–834.
[7] C.M. Chin, R. Paria Sena, E.C. Hunter, J. Hadermann, P.D. Battle, J. Solid State Chem. 251 (2017) 224–232.
[8] Y. Tang, E.C. Hunter, P.D. Battle, R. Paria Sena, J. Hadermann, M. Avdeev, J.M. Cadogan, J. Solid State Chem. 242 (2016) 86–95.
[9] Y.W. Tang, E.C. Hunter, P.D. Battle, M. Hendrickx, J. Hadermann, J.M. Cadogan, Inorg. Chem. 57 (2018) 7438–7445.
[10] E.C. Hunter, P.D. Battle, R. Paria Sena, J. Hadermann, J. Solid State Chem. 248 (2017) 96–103.
[11] F.L. Pratt, Physica B 289 (2000) 710–714.
[12] J.A. Mydosh, Spin Glasses: an Experimental Introduction, Taylor & Francis, London, 1993.
[13] D.X. Chen, V. Skumryev, J.M.D. Coey, Phys. Rev. B 53 (1996) 15014–15022.
[14] D. Gatteschi, R. Sessoli, J. Villain, Molecular Nanomagnets, Oxford Univ Press, New York, 2011.
[15] C.V. Topping, S.J. Blundell, J. Phys. Condens. Matter 31 (2019) 013001.
[16] K.S. Cole, R.H. Cole, J. Chem. Phys. 9 (1941) 341–351.
[17] C.M. Chin, P.D. Battle, A.L. Goodwin, Solid State Chem 278 (2019) 120920.